Intraseasonal Kelvin waves along the southern coast of Sumatra and Java

Iskhaq Iskandar
Department of Earth and Planetary Science, Graduate School of Science, University of Tokyo, Tokyo, Japan

Wijaya Mardiansyah
Department of Physics, Faculty of Mathematics and Natural Science, Sriwijaya University, South Sumatra, Indonesia

Yukio Masumoto and Toshio Yamagata
Department of Earth and Planetary Science, Graduate School of Science, University of Tokyo, Tokyo, Japan

Received 26 May 2004; revised 9 February 2005; accepted 22 February 2005; published 29 April 2005.

[1] The intraseasonal sea level variations along the southern coast of Sumatra and Java are investigated using in situ data and the TOPEX/Poseidon satellite altimetry data. The analysis shows that there are two intraseasonal variations of distinct timescale: 20–40 days during boreal summer (JJA) and 60–90 days during boreal winter (DJF). During boreal summer the shorter time variations of the sea level along the coast of Sumatra and Java are traced back to the eastern equatorial Indian Ocean (EIO); this indicates the importance of the remotely forced equatorial Kelvin waves. During boreal winter, on the other hand, both the remote winds over the EIO and the local alongshore winds are important in explaining the longer time variations of the sea level along the coast. Further analysis indicates that these intraseasonal variations are associated with the coastal Kelvin waves with phase speed ranging from 1.5 to 2.86 m/s. A simple analytical model forced by daily wind stress confirms the above intraseasonal variations along the southern coast of Sumatra and Java.

Citation: Iskandar, I., W. Mardiansyah, Y. Masumoto, and T. Yamagata (2005), Intraseasonal Kelvin waves along the southern coast of Sumatra and Java, *J. Geophys. Res.*, *110*, C04013, doi:10.1029/2004JC002508.

1. Introduction

[2] It is widely accepted that Yoshida-Wyrtki Jet in the Equatorial Indian Ocean (EIO) occurs twice a year during the monsoon transition periods in April/May and October/November. The jet is confined to the equator within a narrow band of a few degrees and flow eastward across the Indian Ocean with a typical surface zonal velocity of about 80 cm/s or more [*Wyrtki*, 1973; *O'Brien and Hurlburt*, 1974]. Once reaching the eastern boundary, the jet bifurcates to the north and south and propagates poleward along the eastern coast of the Indian Ocean as coastal Kelvin waves, but a part of the energy is reflected back into the interior Indian Ocean as Rossby waves [*Clarke and Liu*, 1993, 1994; *Yamagata et al.*, 1996]. Also, the jet influences the oceanic conditions along the eastern coast [*Wyrtki*, 1973; *Clarke and Liu*, 1993], and several authors discussed their possible impact on the Indonesian throughflow [*Yamagata et al.*, 1996; *Masumoto and Yamagata*, 1996; *Arief and Murray*, 1996; *Sprintall et al.*, 2000]. They suggested that the seasonal variations of the Lombok throughflow, one of the major passages of the Indonesian throughflow, are partially governed by the incoming energy from the EIO in terms of the coastal Kelvin waves. Moreover, temperature and sea level variability in the eastern Indian Ocean and the Indonesian seas have been examined using long-term repeat expandable bathythermograph (XBT) data [*Wijffels and Meyers*, 2004]. Their analysis shows that seasonal to interannual variability of the temperature and sea levels in the Indonesian seas is predominantly excited by remote zonal winds along the equator of the Indian and Pacific Oceans. They suggest that some energy from the EIO penetrates into the internal Indonesian seas with an impact on the internal sea level and thermocline depth variability.

[3] Most of the previous studies have been devoted to investigation of the seasonal variability in the EIO using monthly data. Therefore short-term variations from weeks to months are smeared out from the original data. However, our understanding of such short-term variability of the upper EIO has been improved using both direct observations and modeling efforts. Analysis of the observational data showed an energy peak of the zonal flow on the intraseasonal timescale of 30–60 days [*Luyten and Roemmich*, 1982; *McPhaden*, 1982; *Reppin et al.*, 1999; *Webster et al.*, 2002]. Measurement using shallow pressure gauge array (SPGA) in five outflow straits in the eastern Indonesian archipelago demonstrated that the

0148-0227/05/2004JC002508

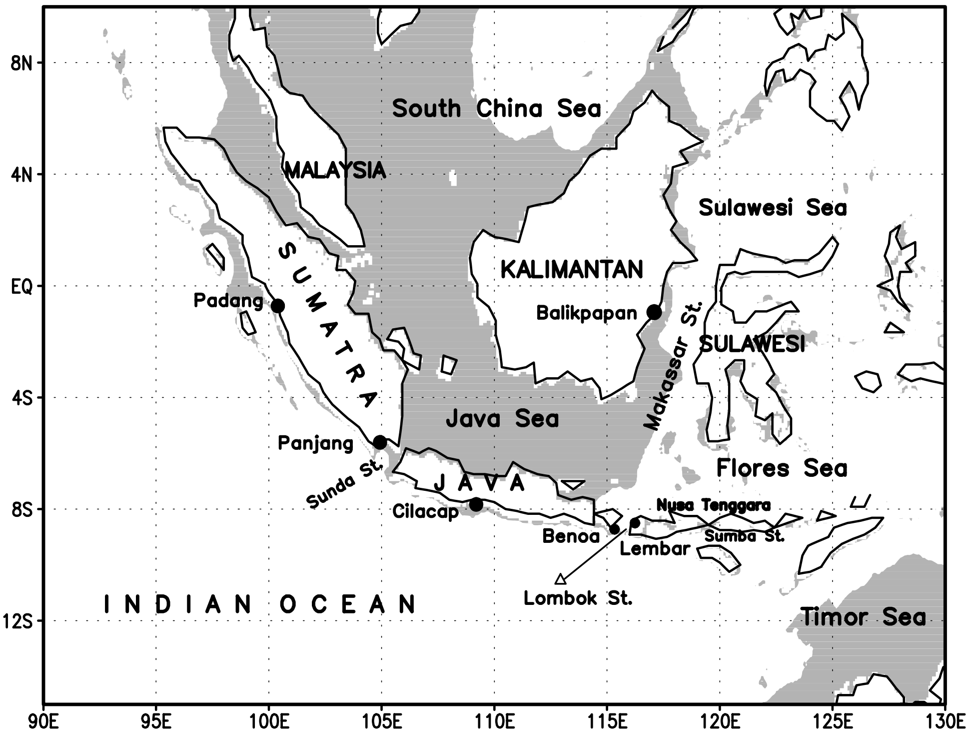

Figure 1. Locations of the tidal stations used in this study. Padang (0°57′S, 100°22′E), Panjang (5°25′S, 105°15′E), Cilacap (7°34′S, 108°59′E), Benoa (8°46′S, 115°13′E), Lembar (8°44′S, 116°05′E), and Balikpapan (1°17′S, 116°48′E). The 200 m isobath is shaded. Courtesy of the National Coordinating Agency for Surveys and Mapping (BAKOSURTANAL), Indonesia.

surface flow fluctuates with period of 30–90 days oscillation [*Chong et al.*, 2000]. This intraseasonal variability is correlated with the remote winds in the eastern EIO and local winds along the Indonesian archipelago. *Potemra et al.* [2002], using the extended SPGA data of *Chong et al.* [2000], showed that the dominant feature of the outflow variability is on the intraseasonal timescale. They also showed that the magnitude decreases as the strait locates further eastward. Furthermore, they proposed that the semiannual variations in monsoonal winds and the Madden-Julian Oscillation (MJO) activity over the EIO are potential candidates to produce the intraseasonal variability.

[4] On the other hand, *Qiu et al.* [1999], using a 1.5-layer reduced gravity model, demonstrated that variations in the southeastern Indian Ocean are characterized by oscillations with periods of 50 and 85 days. *Sengupta et al.* [2001], using a general circulation model, demonstrated intraseasonal variability of surface current in the eastern and central Indian Ocean with a typical period of 30–50 days. *Han et al.* [2001] employed nonlinear and linear 4.5-layer ocean models and confirmed that such shorter time variability (40–60 days) in the zonal current is mainly excited by intraseasonal winds associated with the MJO. Furthermore, *Senan et al.* [2003], using an ocean general circulation model, showed distinct intraseasonal jets in the eastern EIO associated with the intraseasonal oscillation of the boreal summer monsoon.

[5] More recently, an ADCP mooring at 90°E right on the equator clearly shows the existence of intraseasonal equatorial jets in the eastern EIO with a typical period of 30–50 days [*Masumoto et al.*, 2005]. The analysis of the zonal wind stress averaged from 80°E to 90°E along the equator indicates that these intraseasonal jets are forced primarily by the winds associated with the intraseasonal disturbances in the atmosphere.

[6] In this study, we examine the relationship between the intraseasonal sea level variations and the intraseasonal disturbances of the atmospheric winds both over the EIO and along the southern coast of Sumatra and Java. Using various observational data, we discuss intraseasonal Kelvin waves along the southern coast of Sumatra and Java, and show that both remote and local winds are responsible for generating these waves.

[7] This paper is organized as follows. A brief description of the data set used in this study is presented in the next section. In section 3, the wavelet analysis of the observed sea level is used to describe the intraseasonal band. Simple model experiments forced by the wind stress are presented also in this section to discuss possible generation mechanisms of the intraseasonal variability. A summary is given in the final section.

2. Data

[8] We use hourly sea level data recorded at four tidal stations located along the coast of Sumatra and Java and two stations located within the Indonesian seas for the period from January 1995 to April 1997 (Figure 1). The data are checked for errors and datum shifts. Mean sea

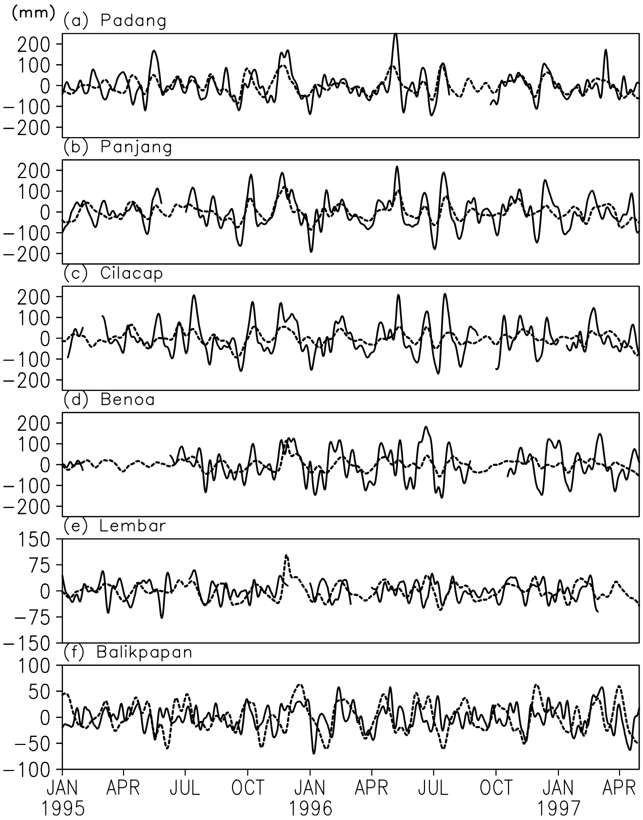

Figure 2. Time series of the sea level anomalies observed by tidal station (solid lines) and TOPEX/Poseidon (dashed lines) after 10–100 days of band-pass filtering.

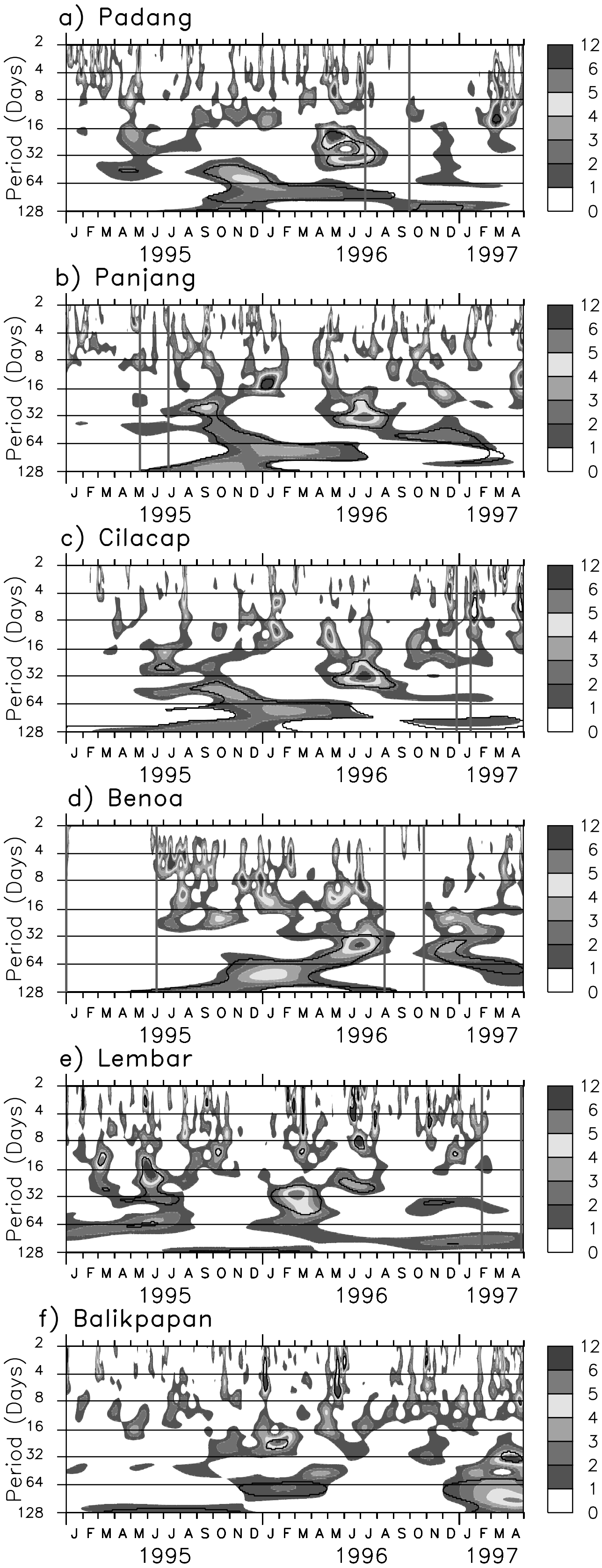

Figure 3. Morlet wavelet spectrum of the observed sea level being normalized by global wavelet spectrum. The thick contours correspond to the 95% confidence level.

level from adjacent time period is used to correct datum shifts when available. Then short gaps of up to 13 days are filled in by applying linear interpolation, but some missing periods of more than 13 days are treated as no data. In order to remove higher-frequency variability associated with semidiurnal and diurnal tides, we applied low-pass filter based on a Butterworth filter [*Emery and Thomson*, 2001, p. 540] with the cut-off period of 48 hours. The hourly data are then simply averaged to obtain daily sea level data and linear trends are removed. Finally, barometric effects are corrected by subtracting the sea level pressure obtained from European Centre for Medium-Range Weather Forecasts (ECMWF) reanalysis data.

[9] The gridded altimeter sea surface height anomalies (SSHA) of the TOPEX/Poseidon are used in this study. Here we use the 1.0°, 5 day interpolated version of the WOCE PODAAC-v3 data set, which is available at http://podaac.jpl.nasa.gov/woce/woce3_topex.

[10] The wind stress data used in this study are based on the daily mean ECMWF reanalysis data. The data cover the whole globe with a spatial resolution of 2.5° in both latitude and longitude. To show the relation between winds and sea level variations, we choose 30 points of the wind stress data: 22 points along the equatorial Indian Ocean and 8 points along the coast of Sumatra and Java. Only the zonal winds are considered along the EIO and along the coast of Java, whereas both zonal and meridional wind components are

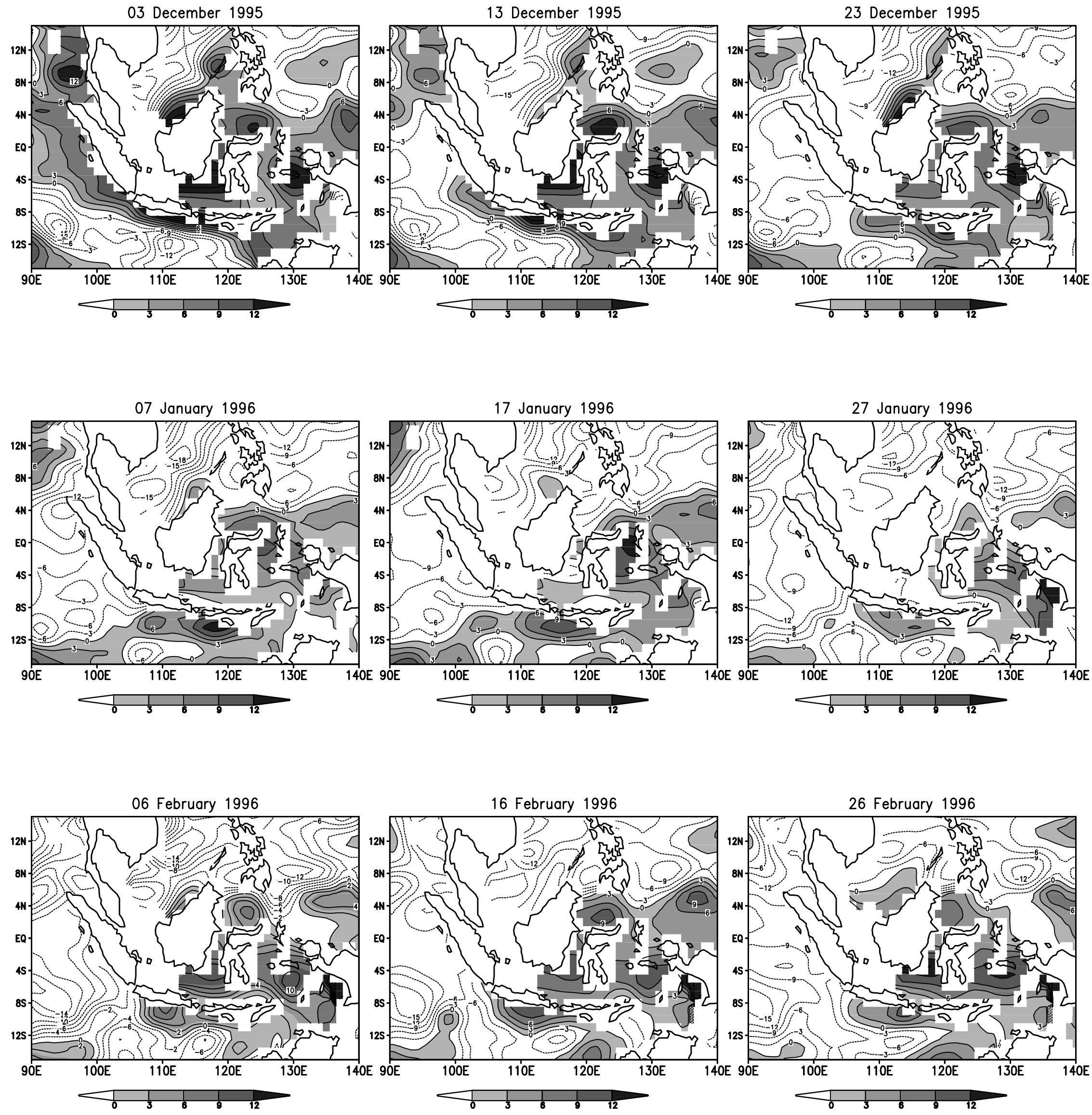

Figure 4. Sea surface height anomaly (SSHA) from TOPEX/Poseidon altimeter during boreal winter (DJF). The SSHA is a deviation from the time mean of 1993–2001. The contour interval is 3 cm, and positive anomalies are shaded.

considered to calculate the alongshore component along the coast of Sumatra.

3. Results

3.1. Intraseasonal Variations

[11] Figure 2 compares the time series of sea level anomalies of the tidal stations and TOPEX/Poseidon altimeter data from January 1995 to April 1997 after 10–100 days band-pass filtering. It is evident from the tidal station data that strong semiannual cycle associated with the classical Yoshida-Wyrtki Jet is observed at all stations along the coast of Sumatra and Java. We note that high-frequency fluctuations are remarkable at Balikpapan located within the Makassar Strait. This is consistent with *Ffield and Gordon*'s [1996] finding that the combination between solar and lunar semidiurnal tides results in fortnightly tidal signal in the Makassar Strait [see also *Susanto et al.*, 2000]. The sea level variability observed at Balikpapan may also be influenced by incoming signals from the Sulawesi Sea [cf. *Susanto et al.*, 2000]. We also note that the sea level fluctuations observed at Lembar are weaker compare to those observed at Benoa. The location of Lembar facing the Flores Sea could possibly explain this discrepancy. *Wijffels and Meyers* [2004] proposed that the Pacific wind forcing related to Rossby wave energy is more dominant in affecting thermocline variability at north of Nusa Tenggara Islands Chain.

[12] In addition to semiannual variations, intraseasonal variations are also remarkable at all stations along the coast of Sumatra and Java. Their amplitude during boreal summer (JJA) is as large as those associated with the classical Yoshida-Wyrtki Jet. We also note that the amplitude of the intraseasonal variations during boreal winter (DJF) increases, as stations are located farther southeastward along the coast.

[13] In order to investigate the dominant frequency of the sea level variations, the wavelet power spectrum analysis

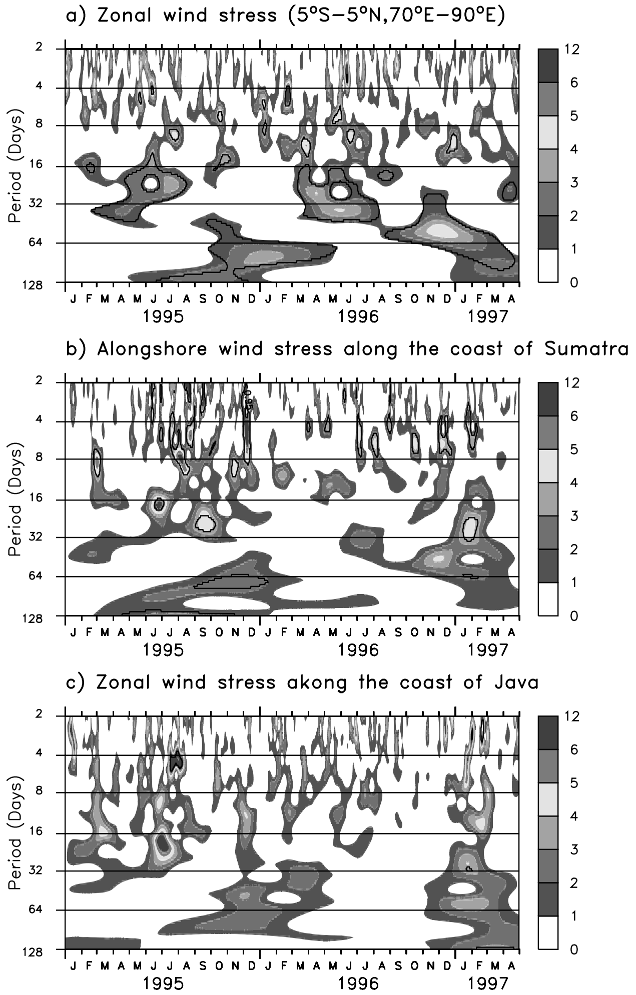

Figure 5. As in Figure 3, except for the remote and the local wind stress.

[*Torrence and Compo*, 1998] is applied on the adjusted sea levels at all stations. We used the Morlet wavelet as the mother wavelet and a red noise background spectrum with autoregressive lag 1 correlation of 0.72 was used to calculate the 95% confidence level. The results normalized by the global wavelet spectrum are presented in Figure 3. The gaps in the records, which are marked by two adjacent red lines, are filled in using the nearest neighbor algorithm prior to the analysis. When we find points being equally spaced around the missing point, the mean value is used for the missing point.

[14] We observe shorter time variability with 20–40 days period during boreal summer at all stations except Balikpapan. This intraseasonal variability propagates southeastward as far as Lembar. Once the signals reach the Lombok Strait, they bifurcate into two parts. One part propagates farther eastward following the coast of Nusa Tenggara Islands Chain to the Sumba Strait. Another part penetrates into the Lombok Strait and turns to the Flores Sea [*Hautala et al.*, 2001; *Wijffels and Meyers*, 2004]. *Wyrtki* [1961] reported a persistent southward flow in the Makassar Strait throughout the year. In some cases, however, drifters released in the Indian Ocean intrude into the Makassar Strait [*Michida and Yoritaka*, 1996].

[15] During boreal winter, lower-frequency fluctuations with period of 60–90 days are observed at all stations located along the coast of Sumatra and Java as far as Benoa. The sea level variations observed at Lembar do not show oscillations of this period. Instead, sea levels at Balikpapan demonstrate intraseasonal oscillations of the period. However, this may due to another reason. The TOPEX/Poseidon altimeter data (Figure 4) shows that positive signals, which originate in the eastern EIO and propagate southeastward along the coast of Sumatra and Java, do not enter the Lombok Strait. Moreover, the intraseasonal fluctuations observed at Balikapapan appear to be affected predominantly by incoming signals from the Sulawesi Sea during this period.

[16] *Clarke and Liu* [1993] suggested that sea level variability along the eastern boundary of the Indian Ocean is driven mainly by the atmospheric winds. To identify what kind of atmospheric forcing is responsible for the sea level oscillations, we apply similar wavelet analysis on both remote winds over the eastern EIO and local winds along the coast of Sumatra and Java. It turns out that the intraseasonal oscillations with a period of 20–40 days during boreal summer exist only in the eastern EIO, indicative of importance of remote wind forcing in explaining intraseasonal sea level variations along the coast of Sumatra and Java (Figure 5). During boreal winter, the intraseasonal oscillations with a period of 60–90 days are found in winds both in the eastern EIO and along the coast of Sumatra and Java, which correspond to the intraseasonal spectra of sea level variations.

[17] To confirm the above relation, we have calculated the correlation between sea level anomaly and zonal wind stress for the 10–100 days band-pass filtered data (Figure 6). The time lag in days is chosen so that we obtain the highest correlation.

[18] It is shown that during boreal summer the observed sea levels show high correlation with the zonal wind stress over the eastern EIO, confirming that remote wind forcing plays an important role in generating sea level variability along the coast. The weak correlation between zonal winds at about 75°E in the equatorial waveguide and the observed sea level at Balikpapan indicates that the latter is less influenced by the former.

[19] During boreal winter both remote winds over the eastern EIO and local winds off Sumatra contribute to the sea level variations at Padang and Panjang (not shown). The local wind forcing off south Java also significantly correlates with the sea level at Cilacap and Benoa during boreal winter. With increasing the time lag, the sea level shows high correlation only with the remote winds over the eastern EIO. The lagged correlation analysis shows that the surface winds at 90°E lead the sea level variations observed at Benoa by about 12 days, which indicates the eastward propagation with phase speed of about 2.9 m/s. This is in good agreement with the result of *Sprintall et al.* [2000] for semiannual Kelvin waves. The sea level variations at Balikpapan appear to be influenced by the winds from the equatorial Pacific Ocean during this period. Thus in the rest of this paper, we do not discuss the sea level variations at Balikpapan as already discussed.

[20] To estimate the phase speed of the eastward propagating signal, we have performed a lagged correlation

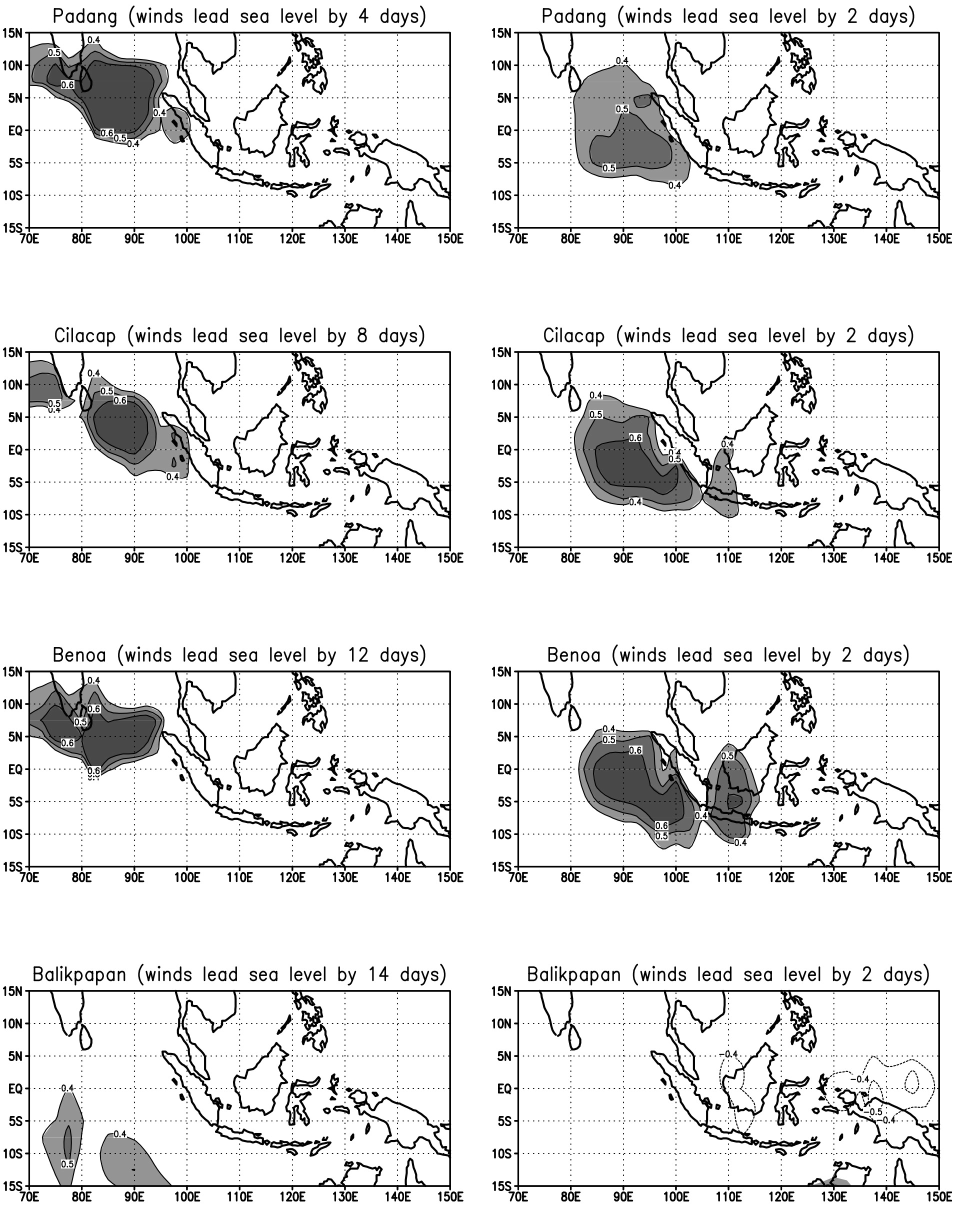

Figure 6. Correlation maps between zonal wind stress and observed sea level for 10–100 days of band-pass filtered data at difference time lag during (left) boreal summer and (right) boreal winter. The 99% significance level is approximately ±0.3.

analysis on the 10–100 days band-pass filtered time series for each station pair (Figure 7). The phase speed thus calculated (except for the correlation between Padang and Panjang) ranges from 1.5 to 2.86 m/s. This suggests the existence of the coastal Kelvin waves, as the speeds are close to the theoretical estimate by *Gill* [1982] and the observed speed by *Wyrtki* [1971]. A broad range of the phase speed suggests effects by ocean currents and/or the wind forcing. *Quadfasel and Cresswell* [1992] and *Sprintall et al.* [1999] showed that the seasonal cycle of the South Java Current (SJC) along the Sunda Islands influences the observed phase speed [cf. *Yamagata et al.*, 1996]. During boreal summer, southeasterly monsoonal winds prevail over the southern Indonesian archipelago, leading to the northwestward SJC along the southern coast of Java. This SJC, in turn, prevents the flow from the EIO from progressing farther eastward. In contrast, during boreal winter the prevailing northwesterly monsoon winds force the SJC southeastward and increase the speed of incoming flow from the eastern EIO. *Quadfasel and Cresswell* [1992] suggested that freshwater from the Sunda Strait and river discharge could also affect the coastal current along the southern coast of Java.

[21] To confirm our analysis based on in situ data, we have also conducted a comparison study using the TOPEX/Poseidon altimeter data (Figure 2). The altimeter data shows a good agreement with the tidal station data; the correlation is high (see Table 1) although the former misses high-frequency fluctuations. This is the inevitable weakness of the TOPEX/Poseidon data. Interestingly, however, the

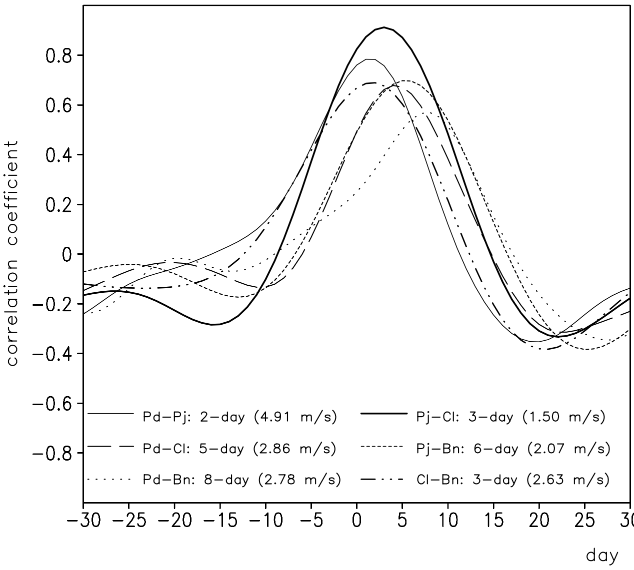

Figure 7. Lagged correlation analysis of 10–100 days of band-pass filtered sea levels. A positive (negative) lag indicates that the variability in a former station leads (lags) that in the latter station. The estimated phase speed between stations pairs are denoted by the values in the parentheses.

TOPEX/Poseidon data captures, to some extent, the intraseasonal variability along the southern coast of Sumatra and Java throughout the whole analysis period; future availability of multiple satellites for altimetry to increase temporal and spatial resolution is highly recommended even for coastal oceanography.

3.2. A Simple Analytical Model

[22] In order to quantify the effect of wind forcing on sea level variations, we adopt a simple analytical model developed by *Gill and Clarke* [1974]. A previous study [*Clarke and Liu*, 1993] showed that the model well resolves semiannual and annual sea level variations along the eastern boundary of the Indian Ocean. *Sprintall et al.* [1999], using a similar model, demonstrated penetration of remotely forced semiannual Kelvin waves into the Indonesian seas during May 1997. We use the first three vertical modes and choose the ECMWF wind stress data for our present purpose of studying the intraseasonal variations. We assume that all of the energy from the EIO propagates southeastward along the coast; it is accepted as the lowest order approximation [see *Clarke and Liu*, 1993].

[23] Introducing the equatorial beta plane and the modal expansion, we drive a simple wave equation to determine sea level changes associated with the equatorial Kelvin wave with a phase speed of c_n. The nondimensional form is

$$\frac{\partial\eta}{\partial t} + \frac{\partial\eta}{\partial x} = X_n, \tag{1a}$$

where

$$X_n = \frac{B_n \tau_n^x}{\rho\left(2\beta c_n^3\right)^{1/2}}. \tag{1b}$$

In the above equation, x refers to the eastward direction. The surface elevation, zonal wind stress, density and time are indicated by η, τ^x, ρ and t, respectively. X_n is the nondimensional zonal wind forcing and $(B_n)^{-1}$ is the equivalent forcing depth. The suffix n denotes the nth vertical mode. The equivalent forcing depth $(B_n)^{-1}$ for the nth vertical mode with the eigenfunction $\psi_n(z)$ is defined by

$$B_n = \frac{\int_{-H_{\rm mix}}^{0} \psi_n dz}{H_{\rm mix}\int_{-H}^{0} \psi_n^2 dz}, \tag{2}$$

Table 1. Correlation Coefficients Between Observed Sea Level Data and Model Results[a]

Station	TS – TP	TS(TP) – MAll	TS(TP) – MIO	TS(TP) – MSJ
Padang	0.59	0.39 (0.75)	0.39 (0.75)	0.11[b] (0.40)
Panjang	0.83	0.67 (0.78)	0.63 (0.73)	0.32 (0.44)
Cilacap	0.66	0.63 (0.71)	0.47 (0.57)	0.49 (0.58)
Benoa	0.68	0.70 (0.70)	0.52 (0.53)	0.46 (0.59)
Lembar	0.46	0.22 (0.73)	0.20 (0.52)	0.11[b] (0.54)

[a]The 99% significance level is approximately ±0.12. TS, tidal station; TP, TOPEX/Poseidon; MAll, model forced by both remote and local winds; MIO, model forced by remote winds; MSJ, model forced by local winds.
[b]Correlations below the significance level.

Table 2. Parameters Used for the Numerical Simulation

Parameter	Mode 1	Mode 2	Mode 3
Phase speed (c_n), m/s	3.03	1.85	1.11
Equivalent depth (B_n^{-1}), m^{-1}	3.08×10^{-3}	1.98×10^{-3}	1.03×10^{-3}
Mixed-layer depth ($H_{\rm mix}$), m	75	75	75

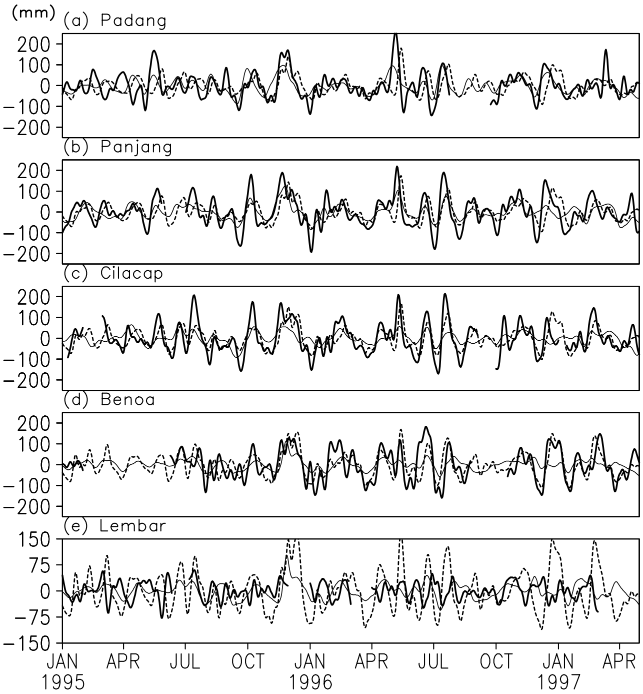

Figure 8. Time series of the sea level anomalies after 10–100 days of band-pass filtering from tidal station (bold line), TOPEX/Poseidon (thin line), and model result forced by both the remote and the local wind forcing (dashed line).

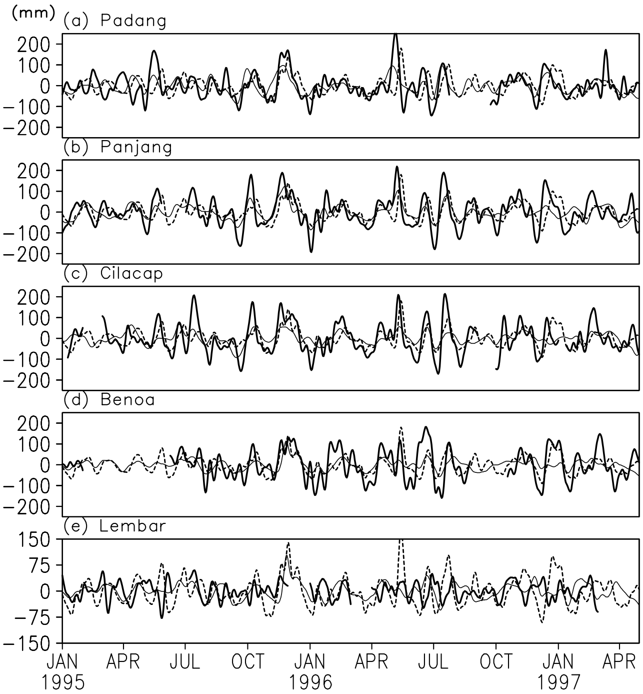

Figure 9. As in Figure 8, except for results from the model forced by remote winds.

where H_{mix} is the mixed layer depth. Introducing a new coordinate system translating with the wave speed, we obtain

$$\frac{\partial \eta}{\partial \xi} = X_n\left(\xi, s + \frac{x}{c_n}\right), \qquad (3)$$

where $s = t - x/c_n$ and $\xi = x$. The sea level changes are calculated using (3) by integrating the modified wind stress along the propagation path.

[24] The vertical mode eigenfunction $\psi_n(z)$ and the corresponding eigenvalue c_n are calculated using *Conkright et al.* [2002]. Used in the calculation is the buoyancy frequency averaged along the propagation path of the Kelvin waves from western Indian Ocean to the Lombok Strait. Parameters used in the calculation are listed in Table 2.

[25] We conduct experiments with three different types of wind forcing. In the first experiment, we incorporate both remote (along the EIO) and the local (along the southern coast of Sumatra, Java to the Lombok Strait) wind forcing. On the other hand, the second and third experiments consider only either the remote or the local wind forcing. These experiments are designed to quantify the effect of the remote and the local forcing on the sea level variability.

[26] Figure 8 compares three time series from each tidal station, TOPEX/Poseidon satellite altimetry and the first experiment. The model sea level variability shows a good agreement with the tidal station data and the TOPEX/Poseidon data (see Table 1). This result suggests that the sea level variations along the southern coast of Sumatra and Java are mostly forced by the atmospheric winds both over the EIO and along the coast. Note that there are large discrepancies at Lembar, where the model signal is larger than the observed one. This may be attributed to the resolution of the wind stress as well as the location of the station at the northern coast of Nusa Tenggara Islands as already discussed.

[27] Comparison with the experiment using either the remote or the local wind forcing (Figures 9 and 10) shows that the intraseasonal variations during boreal summer (JJA) are primarily excited by the remote wind forcing over the EIO. In contrast, during boreal winter (DJF), both the remote and the local wind forcing are responsible for producing positive signals along the southern coast of Java as far as Benoa. The sea level variations along the southern coast of Sumatra, on the other hand, are mainly excited by the wind forcing over the EIO (see Table 1). These results are consistent with the wavelet analysis of both the observed sea level and the surface wind (Figures 3 and 5).

3.3. Basin-Wide Evolution of the Intraseasonal Variability

[28] For further understanding of the intraseasonal variability revealed in the previous subsections, we explore basin-wide TOPEX/Poseidon data and surface winds. Figures 11 and 12 show the time-space diagram of the SSHA from TOPEX/Poseidon data and the surface wind stress from ECMWF reanalysis data after 20–90 days band-pass filtering, respectively. The horizontal axis indicates the distance along the EIO from the west to the east, and then southeastward following the coastline of

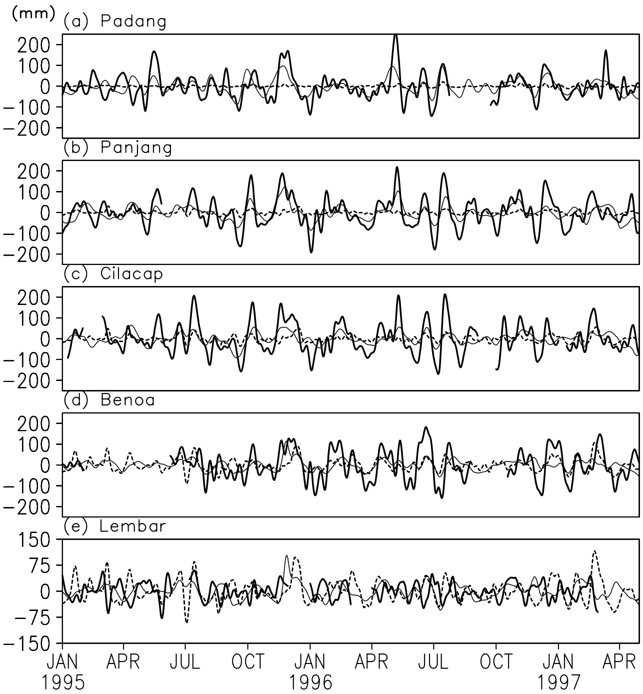

Figure 10. As in Figure 8, except for results from the model forced by local winds.

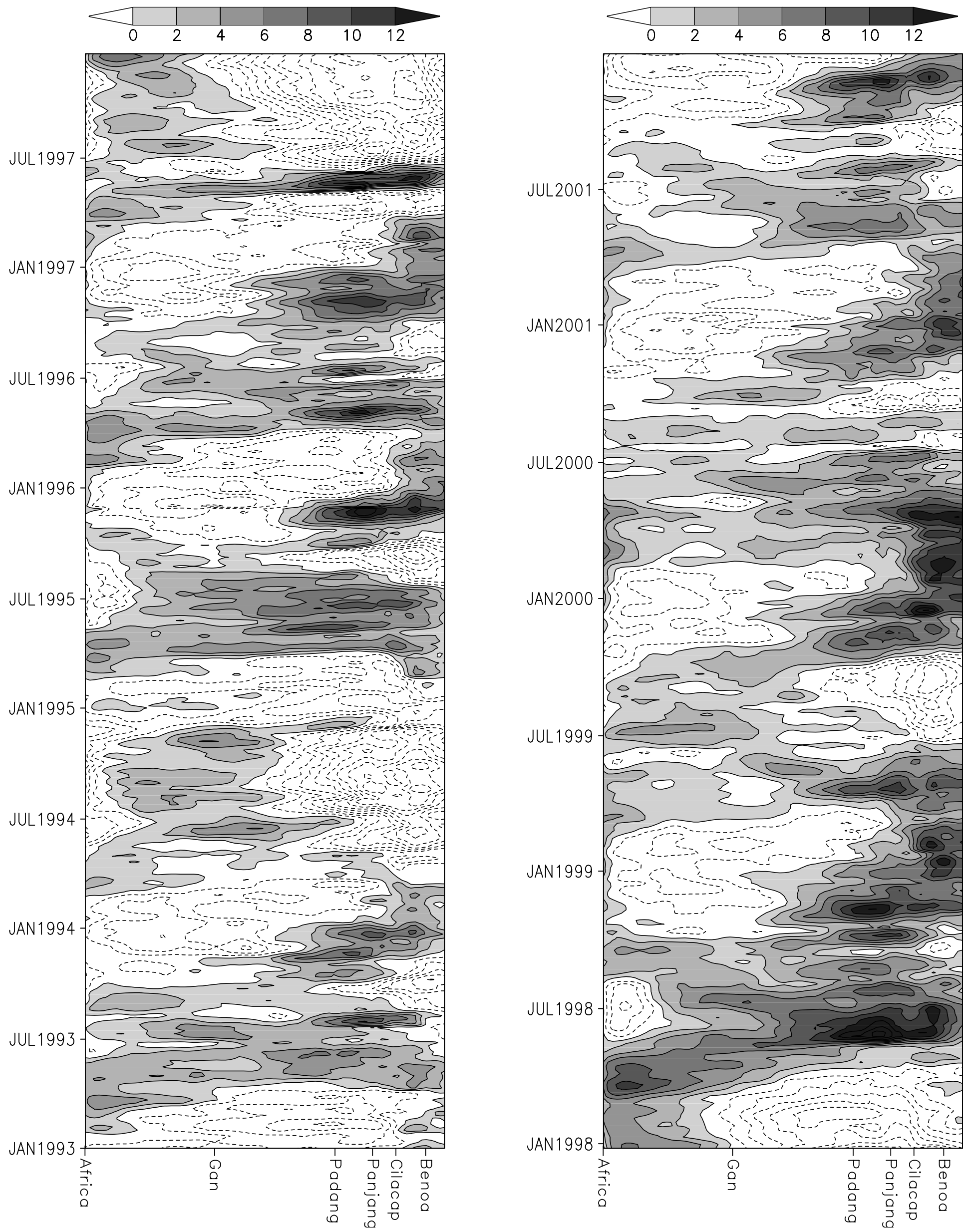

Figure 11. Time-distance diagrams of 20–90 days of band-pass filtered SSHA from TOPEX/Poseidon data during 1993–2001. The contour interval is 2 cm, and high sea levels are shaded.

Sumatra, Java to the Nusa Tenggara Islands chain close to the Lombok Strait.

[29] It is evident from those figures that the intraseasonal variations show seasonal dependence. During boreal summer (JJA), the positive sea level anomalies along the coast of Sumatra and Java are traced back to the eastern EIO, which indicates the importance of the remotely forced downwelling Kelvin waves. In the early June, the westerly winds over the EIO start to develop and trigger the downwelling equatorial Kelvin waves. Subsequently, they generate coastal Kelvin waves once they impinge on the west coast of Sumatra. Most of the resulted coastal Kelvin waves propagate southeastward along the coast [*Clarke and Liu*, 1993]. In contrast, the local winds associated with the boreal summer monsoon are upwelling favorable and tend to reduce the incoming positive signal from the equatorial region. A weakening of the westerly winds over the eastern EIO at the end of June results in a lowering sea level along the coast. This is augmented by the effect of local southeasterly winds, which induces offshore Ekman flow. In early July, the westerly winds over the eastern EIO again start to develop. The coastal Kelvin waves generated by remote winds in August are weakened upon reaching the western coast of Java as the local southeasterly winds that favor coastal upwelling reach the peak phase in August in the western Java [*Yamagata et al.*, 1996]. *Senan et al.* [2003] have suggested that intraseasonal jets in the EIO during boreal summer are driven by intraseasonal westerly wind bursts (10–40 days) during June–July. Our simple model

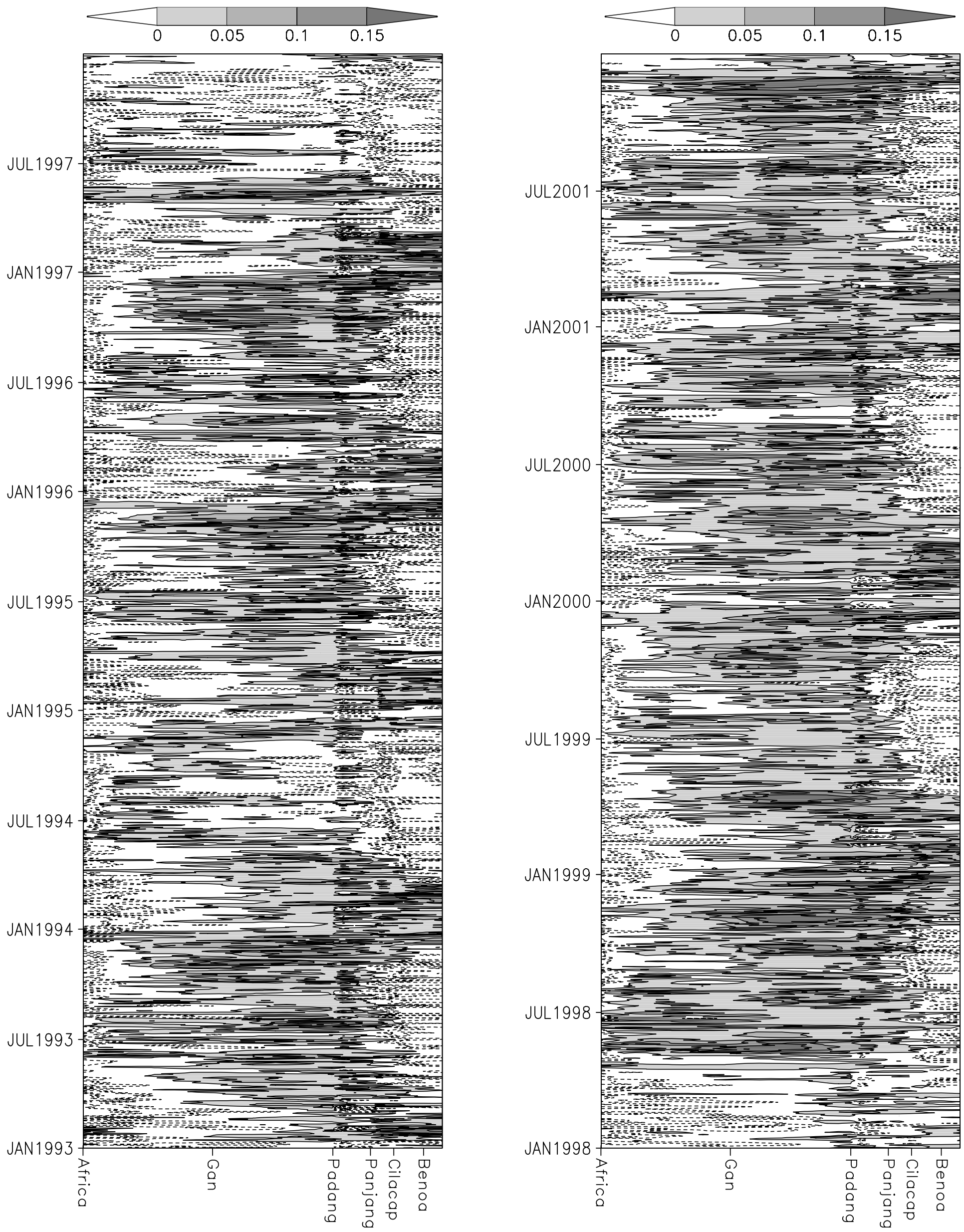

Figure 12. As in Figure 11, except for the daily wind stress from European Centre for Medium-Range Weather Forecasts reanalysis data during 1993–2001. The contour interval is 0.05 dyne cm^{-2}, and westerly winds are shaded.

forced by the remote wind forcing also confirms that the remote forcing is more dominant in producing positive sea level anomalies along the coast during boreal summer (Figure 9).

[30] During boreal winter (DJF), the local alongshore winds blow southeastward with a consequent rise of sea level along the coast due to local Ekman downwelling in the Southern Hemisphere. This effect enhances the remotely forced downwelling Kelvin waves generated by westerly wind bursts in early December in the eastern EIO. In January–February, only weak westerly winds blow over the EIO and do not generate prominent equatorial jets. However, the SSHA at the southern tip of Sumatra coast and along the southern coast of Java show frequent positive anomalies propagating to the east. *Arief and Murray* [1996] attributed the episodic northward flow in the Lombok Strait during February–April to the remotely generated coastal Kelvin waves, which propagate along the southern coast of the archipelago. Further, *Potemra et al.* [2002] suggested that the intraseasonal atmospheric winds in the EIO associated with the MJO are responsible for positive pressure variations observed at Bali during December–February. However, *Chong et al.* [2000] demonstrated that the local alongshore winds are more significant than the remote winds to produce intraseasonal variations in the Lombok Strait throughflow. The results of our simple model forced by either remote or local winds forcing (Figures 9 and 10)

show that both remote and local winds are necessary to explain positive signals along the southern coast of Java during boreal winter.

[31] In summary, the intraseasonal variations in sea level during boreal summer (JJA) are remotely forced by the intraseasonal atmospheric winds over the eastern EIO through the generation of coastal Kelvin waves. The local alongshore winds during this period are upwelling favorable and reduce the incoming signal from the equator. During boreal winter (DJF), on the other hand, both remote and local winds contribute to the sea level variations along the southern coast of Indonesian archipelago. The local winds are downwelling favorable and tend to strengthen the remotely forced downwelling Kelvin waves.

4. Summary

[32] We have investigated the intraseasonal sea level variations with a typical period of 20–40 days and 60–90 days using mostly in situ data obtained along the southern coast of Sumatra and Java. The analysis indicates that the phase speed of the southeastward propagating signal ranges from 1.5 to 2.86 m/s except along the coast of Sumatra. This is in accord with the theoretical value given by *Gill* [1982] and the observed value for the internal Kelvin waves [*Wyrtki*, 1971], suggesting that this intraseasonal variability is associated with the Kelvin waves. The TOPEX/Poseidon altimetry data shows that the intraseasonal variation associated with the downwelling coastal Kelvin waves has strong seasonal dependence. During boreal summer, intraseasonal atmospheric disturbances only over the EIO play a dominant role in exciting the positive sea level anomalies along the observational sites. During boreal winter, however, both the remote winds over the EIO and the local alongshore winds are favorable in forcing the positive fluctuations of the sea level. The simple analytical model result further confirmed our analysis. Therefore we suggest that both remote and local wind forcings are necessary to explain the intraseasonal variability along the southern coast of Sumatra and Java.

[33] In addition, it is quite interesting to clarify possible mechanism of interaction between the intraseasonal variability and the large-scale climate variability, such as Indian Ocean Dipole (IOD). Moreover, there are also unresolved issues related to the link between the intraseasonal variability and the annual variations, particularly through interaction with the seasonally reversing ocean current systems in south Java. A detailed study using a high-resolution OGCM run by the Earth Simulator with a realistic topography is under progress to further enhance our understanding of those interesting issues.

[34] **Acknowledgments.** The authors would like to thank T. Tozuka for his kind and useful comments during the course of this work. Thanks are extended to Y. Niwa, S.A. Rao, and Y. Miyazawa and also to K. Maiwa for their kind assistance in computations. The wavelet software was provided by C. Torrence and G. Compo and is available at http://paos.colorado.edu/research/wavelets. Useful comments provided by two anonymous reviewers helped us to improve the earlier manuscripts. The sea level data are provided by the National Agency for Surveys and Mapping (BAKOSURTANAL), Indonesia. The first author has been supported by the scholarship for foreign students offered by Ministry of Education, Culture, Sports, Science and Technology, Japan.

References

Arief, D., and S. P. Murray (1996), Low-frequency fluctuations in the Indonesian throughflow through Lombok Strait, *J. Geophys. Res.*, *101*, 12,455–12,464.

Chong, J. C., J. Sprintall, S. Hautala, W. L. Morawitz, N. A. Bray, and W. Pandoe (2000), Shallow throughflow variability in the outflow straits of Indonesia, *Geophys. Res. Lett.*, *27*, 125–128.

Clarke, A. J., and X. Liu (1993), Observations and dynamics of semi-annual and annual sea levels near the eastern equatorial Indian Ocean boundary, *J. Phys. Oceanogr.*, *23*, 386–399.

Clarke, A. J., and X. Liu (1994), Interannual sea level in the northern and eastern Indian Ocean, *J. Phys. Oceanogr.*, *24*, 1224–1235.

Conkright, M. E., R. A. Locarnini, H. E. Garcia, T. D. O'Brien, T. P. Boyer, C. Stephens, and J. I. Antonov (2002), *World Ocean Atlas 2001: Objective Analyses, Data Statistics, and Figures* [CD-ROM], Natl. Oceanogr. Data Cent., Silver Spring, Md.

Emery, W. J., and R. E. Thomson (2001), *Data Analysis Methods in Physical Oceanography*, 2nd ed., 638 pp., Elsevier, New York.

Ffield, A., and A. L. Gordon (1996), Tidal mixing signatures in the Indonesian seas, *J. Phys. Oceanogr.*, *26*, 1924–1937.

Gill, A. E. (1982), *Atmosphere-Ocean Dynamics*, *Int. Geophys. Ser.*, vol. 30, 662 pp., Elsevier, New York.

Gill, A. E., and A. J. Clarke (1974), Wind-induced upwelling, coastal currents and sea-level changes, *Deep Sea Res.*, *21*, 325–345.

Han, W., D. M. Lawrence, and P. J. Webster (2001), Dynamical response of equatorial Indian Ocean to intraseasonal winds: Zonal flow, *Geophys. Res. Lett.*, *28*, 4215–4218.

Hautala, S. L., J. Sprintall, J. T. Potemra, J. C. Chong, W. Pandoe, N. Bray, and A. G. Ilahude (2001), Velocity structure and transport of the Indonesian Throughflow in the major straits restricting flow into the Indian Ocean, *J. Geophys. Res.*, *106*, 19,527–19,546.

Luyten, J. R., and D. Roemmich (1982), Equatorial currents at semiannual period in the Indian Ocean, *J. Phys. Oceanogr.*, *12*, 406–413.

Masumoto, Y., and T. Yamagata (1996), Seasonal variations of the Indonesian throughflow in a general ocean circulation model, *J. Geophys. Res.*, *101*, 12,287–12,293.

Masumoto, Y., H. Hase, Y. Kuroda, H. Matsuura, and K. Takeuchi (2005), Intraseasonal variability in the upper-layer currents observed in the eastern equatorial Indian Ocean, *Geophys. Res. Lett.*, *32*, L02607, doi:10.1029/2004GL021896.

McPhaden, M. J. (1982), Variability in the central equatorial Indian Ocean. Part 1: Ocean dynamics, *J. Mar. Res.*, *40*, 157–176.

Michida, Y., and H. Yoritaka (1996), Surface currents in the area of the Indo-Pacific throughflow and in the tropical Indian Ocean observed with surface drifters, *J. Geophys. Res.*, *101*, 12,475–12,482.

O'Brien, J. J., and H. E. Hurlburt (1974), Equatorial jet in the Indian Ocean: Theory, *Science*, *184*, 1075–1077.

Potemra, J. T., S. L. Hautala, J. Sprintall, and W. Pandoe (2002), Interaction between the Indonesian seas and the Indian Ocean in observations and numerical models, *J. Phys. Oceanogr.*, *32*, 1838–1854.

Qiu, B., M. Mao, and Y. Kashino (1999), Intraseasonal variability in the Indo-Pacific throughflow and regions surrounding the Indonesian seas, *J. Phys. Oceanogr.*, *29*, 1599–1618.

Quadfasel, D. R., and G. Cresswell (1992), A note on the seasonal variability of the south Java current, *J. Geophys. Res.*, *97*, 3685–3688.

Reppin, J., F. A. Schott, J. Fischer, and D. Quadfasel (1999), Equatorial currents and transports in the upper central Indian Ocean: Annual cycle and interannual variability, *J. Geophys. Res.*, *104*, 15,495–15,514.

Senan, R., D. Sengupta, and B. N. Goswami (2003), Intraseasonal "monsoon jets" in the equatorial Indian Ocean, *Geophys. Res. Lett.*, *30*(14), 1750, doi:10.1029/2003GL017583.

Sengupta, D., R. Senan, and B. N. Goswami (2001), Origin of intraseasonal variability of circulation in the tropical central Indian Ocean, *Geophys. Res. Lett.*, *28*, 1267–1270.

Sprintall, J., J. Chong, F. Syamsudin, W. Morawitz, S. Hautala, N. Bray, and S. Wijffels (1999), Dynamics of the South Java Current in the Indo-Australian Basin, *Geophys. Res. Lett.*, *26*, 2493–2496.

Sprintall, J., A. L. Gordon, R. Murtugudde, and R. Dwi Susanto (2000), A semiannual Indian Ocean forced Kelvin wave observed in the Indonesian seas in May 1997, *J. Geophys. Res.*, *105*, 17,217–17,230.

Susanto, R. D., A. L. Gordon, J. Sprintall, and B. Herunadi (2000), Intraseasonal variability and tides in Makassar Strait, *Geophys. Res. Lett.*, *27*, 1499–1502.

Torrence, C., and G. P. Compo (1998), A practical guide to wavelet analysis, *Bull. Am. Meteorol. Soc.*, *79*, 61–78.

Webster, P. J., et al. (2002), The JASMINE pilot study, *Bull. Am. Meteorol. Soc.*, *11*, 1603–1630.

Wijffels, S., and G. Meyers (2004), An interaction of oceanic waveguides: Variability in the Indonesian throughflow region, *J. Phys. Oceanogr.*, *34*, 1232–1253.
Wyrtki, K. (1961), Physical oceanographic of the Southeast Asian waters: Scientific results of marine investigations of the South China Sea and the Gulf of Thailand 1959–1960, *NAGA Rep. 2*, 195 pp., Scripps Inst. of Oceanogr., La Jolla, Calif.
Wyrtki, K. (1971), Oceanographic atlas of the international Indian Ocean Expedition, *Publ. NSF-IDOE-1*, 531 pp., Natl. Sci. Found., Washington, D. C.
Wyrtki, K. (1973), An equatorial jet in the Indian Ocean, *Science*, *181*, 262–264.
Yamagata, T., K. Mizuno, and Y. Masumoto (1996), Seasonal variations in the equatorial Indian Ocean and their impact on the Lombok throughflow, *J. Geophys. Res.*, *101*, 12,465–12,473.

I. Iskandar, Y. Masumoto, and T. Yamagata, Department of Earth and Planetary Science, Graduate School of Science, University of Tokyo, 7-3-1 Hongo, Bunkyo-ku, Tokyo 113-0033, Japan. (iskhaq@eps.s.u-tokyo.ac.jp; masumoto@eps.s.u-tokyo.ac.jp; yamagata@eps.s.u-tokyo.ac.jp)
W. Mardiansyah, Department of Physics, Faculty of Mathematics and Natural Science, Sriwijaya University, Indralaya, OI, South Sumatra 30662, Indonesia. (wmardiansyah@unsri.ac.id)